PLOS ONE

RESEARCH ARTICLE

A Nano-MgO and Ionic Liquid-Catalyzed 'Green' Synthesis Protocol for the Development of Adamantyl-Imidazolo-Thiadiazoles as Anti-Tuberculosis Agents Targeting Sterol 14α-Demethylase (CYP51)

Sebastian Anusha[1], Baburajeev CP[1], Chakrabhavi Dhananjaya Mohan[2], Jessin Mathai[3], Shobith Rangappa[4], Surender Mohan[5], Chandra[6], Shardul Paricharak[7,8], Lewis Mervin[7], Julian E. Fuchs[7], Mahedra M[6], Andreas Bender[7], Basappa[1]*, Kanchugarakoppal S. Rangappa[2]*

1 Laboratory of Chemical Biology, Department of Chemistry, Bangalore University, Central College campus, Palace Road, Bangalore, 560 001, India, **2** Department of Studies in Chemistry, University of Mysore, Manasagangotri, Mysore, 570 006, India, **3** Centre for Advanced Biomedical Research and Innovation, Gulf Medical University, Ajman, United Arab Emirates, **4** Frontier Research Center for Post-genome Science and Technology, Hokkaido University, Sapporo, 060–0808, Japan, **5** Laboratory of Molecular Biology and Genetic Engineering, School of Biotechnology, Jawaharlal Nehru University, New Delhi, 110067, India, **6** Department of Studies in Physics, University of Mysore, Manasagangotri, Mysore, 570 006, India, **7** Centre for Molecular Informatics, Department of Chemistry, University of Cambridge, Lensfield Road, CB2 1EW, Cambridge, United Kingdom, **8** Division of Medicinal Chemistry, Leiden Academic Centre for Drug Research, Leiden University, P.O. Box 9502, 2300, RA Leiden, The Netherlands

* salundibasappa@gmail.com (B); rangappaks@yahoo.com (KSR)

OPEN ACCESS

Citation: Anusha S, CP B, Mohan CD, Mathai J, Rangappa S, Mohan S, et al. (2015) A Nano-MgO and Ionic Liquid-Catalyzed 'Green' Synthesis Protocol for the Development of Adamantyl-Imidazolo-Thiadiazoles as Anti-Tuberculosis Agents Targeting Sterol 14α-Demethylase (CYP51). PLoS ONE 10(10): e0139798. doi:10.1371/journal.pone.0139798

Editor: Firas H Kobeissy, University of Florida, UNITED STATES

Received: June 18, 2015

Accepted: September 17, 2015

Published: October 15, 2015

Data Availability Statement: CCDC NO.1056579 contains the supplementary crystallographic data for this paper. These data can be obtained free of charge at www.ccdc.cam.ac.uk/conts/retrieving.html [or from the Cambridge Crystallographic Data Centre (CCDC), 12 Union Road, Cambridge CB2 1EZ, UK; fax: +44(0) 1223 762911; email: deposit@ccdc.cam.ac.uk].

Funding: This research was supported by University Grants Commission (41-257-2012-SR), Vision Group Science and Technology, Department of Science and

Abstract

In this work, we describe the 'green' synthesis of novel 6-(adamantan-1-yl)-2-substituted-imidazo[2,1-b][1,3,4]thiadiazoles (AITs) by ring formation reactions using 1-(adamantan-1-yl)-2-bromoethanone and 5-alkyl/aryl-2-amino1,3,4-thiadiazoles on a nano material base in ionic liquid media. Given the established activity of imidazothiadiazoles against *M*. *tuberculosis*, we next examined the anti-TB activity of AITs against the H_{37}Rv strain using Alamar blue assay. Among the tested compounds 6-(adamantan-1-yl)-2-(4-methoxyphenyl)imidazo[2,1-b][1,3,4]thiadiazole (**3f**) showed potent inhibitory activity towards *M*. *tuberculosis* with an MIC value of 8.5 μM. The inhibitory effect of this molecule against *M*. *tuberculosis* was comparable to the standard drugs such as Pyrazinamide, Streptomycin, and Ciprofloxacin drugs. Mechanistically, an *in silico* analysis predicted sterol 14α-demethylase (CYP51) as the likely target and experimental activity of **3f** in this system corroborated the *in silico* target prediction. In summary, we herein report the synthesis and biological evaluation of novel AITs against *M*. *tuberculosis* that likely target CYP51 to induce their antimycobacterial activity.

Technology (NO. SR/FT/LS-142/2012). KSR thanks Institution of Excellence, University of Mysore for funding. AB thanks Unilever and the European Research Commission (ERC Starting Grant 2013) for funding. SP thanks the Netherlands Organization for Scientific Research (NWO, grant number NWO-017.009-065) and the Prins Bernhard Cultuurfonds for funding. CDM thanks University of Mysore for Department of Science and Technology-Promotion of University Research and Scientific Excellence (DST-PURSE) Research Associate fellowship.

Competing Interests: The authors have the following interests. This study was partly supported by Unilever. There are no patents, products in development or marketed products to declare. This does not alter the authors' adherence to all the PLOS ONE policies on sharing data and materials, as detailed online in the guide for authors.

Introduction

Tuberculosis (TB) is one of the leading contagious and airborne disease caused by *Mycobacterium tuberculosis* [1, 2] and according to 2013 report of World Health Organization, TB stands second in terms of global mortality from a single infectious agent with 1.5 million death in 2013 worldwide. The conventional TB treatment comprises a cocktail of first-line drugs, namely isoniazid, pyrazinamide, ethambutol and rifampicin which are associated with lowered efficacy due to resistance development and severe adverse effects [3, 4]. The subsequent use of second-line drugs were also reported to suffer from similar problems [5–7]. Gradual increase of multidrug and extensively drug resistant (XDR-TB) mycobacterial strains demands the need of new therapeutic agents which can effectively target TB. The presence of lipid-rich cell surface on mycobacterium provides an effective therapeutic target to design anti-TB agents [8]. Researchers have rightly called adamantanyl ring as 'lipophilic bullet' which effectively targets mycobacterium. Evidently, hybrid obtained from the coupling of adamantylacetamide ring with 1,2,3-triazoles resulted in development of potent inhibitors against *M. tuberculosis* [2]. Adamantyl urea derivatives were reported to induce antimycobacterial action against *M. tuberculosis* [9]. SQ109, an adamantane based small molecule which is in phase-II clinical trials for the treatment of pulmonary TB [10–12]. On the other hand, Delamanid, an imidazo-oxazole based anti-tuberculosis drug was approved for the treatment of multidrug-resistant tuberculosis [13]. Thiadiazoles and imidazothiadiazoles were reported to have antitubercular activity against *M. tuberculosis* $H_{37}Rv$ strains [14–16]. Based on these reports, we attempted to tether the imidazo-thiadiazole nuclei to adamantyl ring in order to enhance the bioactivity profile of the newer drug-seeds. We previously developed several heterocycle based small molecules and explored the various pharmacological properties [17–25]. In the present report, we synthesized a series of novel adamantanyl-tethered imidazo-thiadiazoles for the first-time and evaluated for their inhibitory activity towards *M. tuberculosis*, and a subsequent mode-of-action analysis identified that they likely achieve this activity by targeting sterol 14α-demethylase (CYP51) (S1 Data).

Results and Discussion

Chemistry

The reaction between 1-(adamantan-1-yl)-2-bromoethanone and 5-substitued-2-amino-1,3,4-thiadiazoles yielded 6-(adamantan-1-yl)-2-substituted-imidazo[2,1-b][1,3,4]thiadiazoles ('AITs') with varying yields under different base and solvent conditions (Fig 1A, Scheme 1). Use of solvents such as ethanol, 1-butanol, N,N-dimethyl formamide resulted in poor yields. In order to overcome yield limitation, we next used various ionic liquids (ILs) in combination with a nano-catalyst, nano-MgO (Table 1) [26, 27]. ILs are molten salts, which can dramatically accelerate the rate of reactions, and have often been found to be a suitable substitute for low-boiling organic solvents in terms of toxicity, volatility and flammability [28]. In addition, ILs have more favorable 'green' properties, since they are reusable. In the current work, replacement of organic solvents with ILs significantly improved yields of the product to greater than 90%. In particular, $[BMIM]^+[BF_4]^-$ and $[BMPy]^+[PF_6]^-$ were found to be the better ILs and we have chosen $[BMIM]^+[BF_4]^-$ for the preparation of compounds due to its solubility in water. Additionally, this method was found to be green protocol for the preparation of alkyl or aryl substitution on thiadiazole ring (Table 2). All the isolated products of the reaction were fully characterized by ^1H NMR, LC-MS and elemental analysis. Finally, we prepared the single crystal of one of the AITs, namely **3b**, *via* slow evaporation technique. The single crystal X-ray diffraction studies of **3b** confirmed formation of the title compounds (Fig 1B).

Figure 1

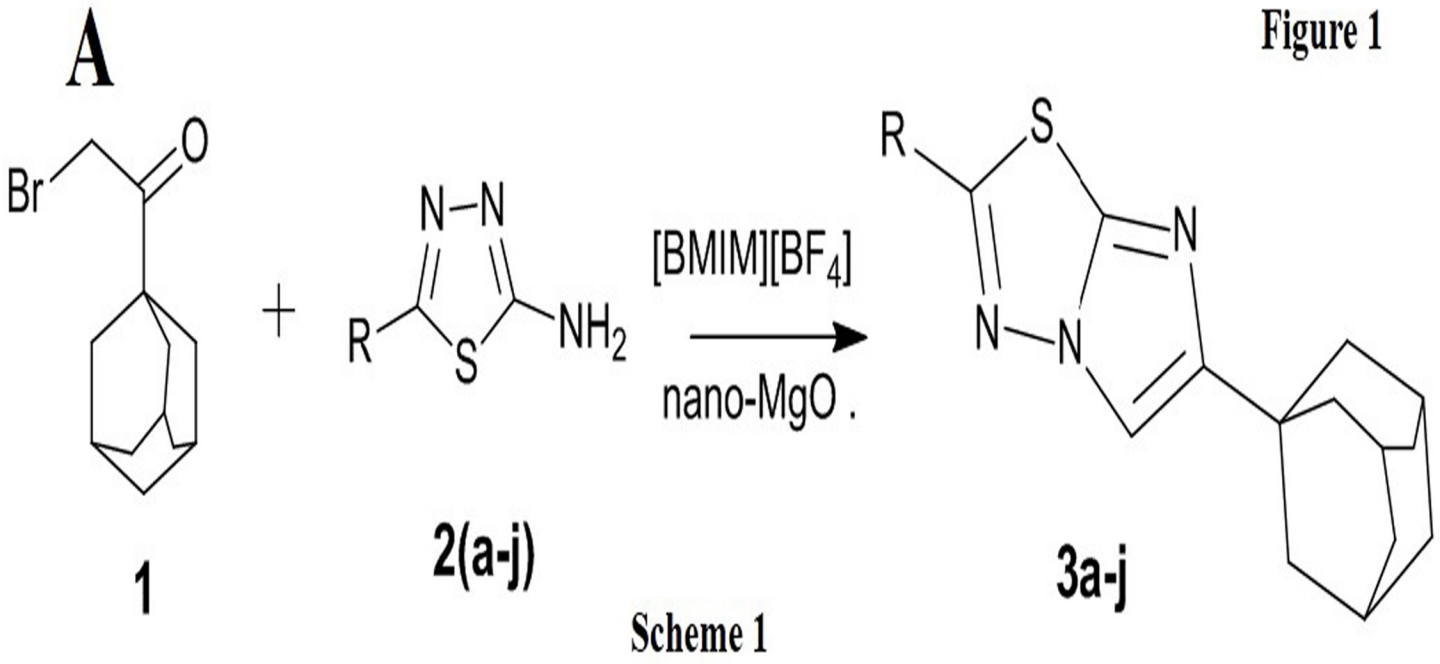

Scheme 1

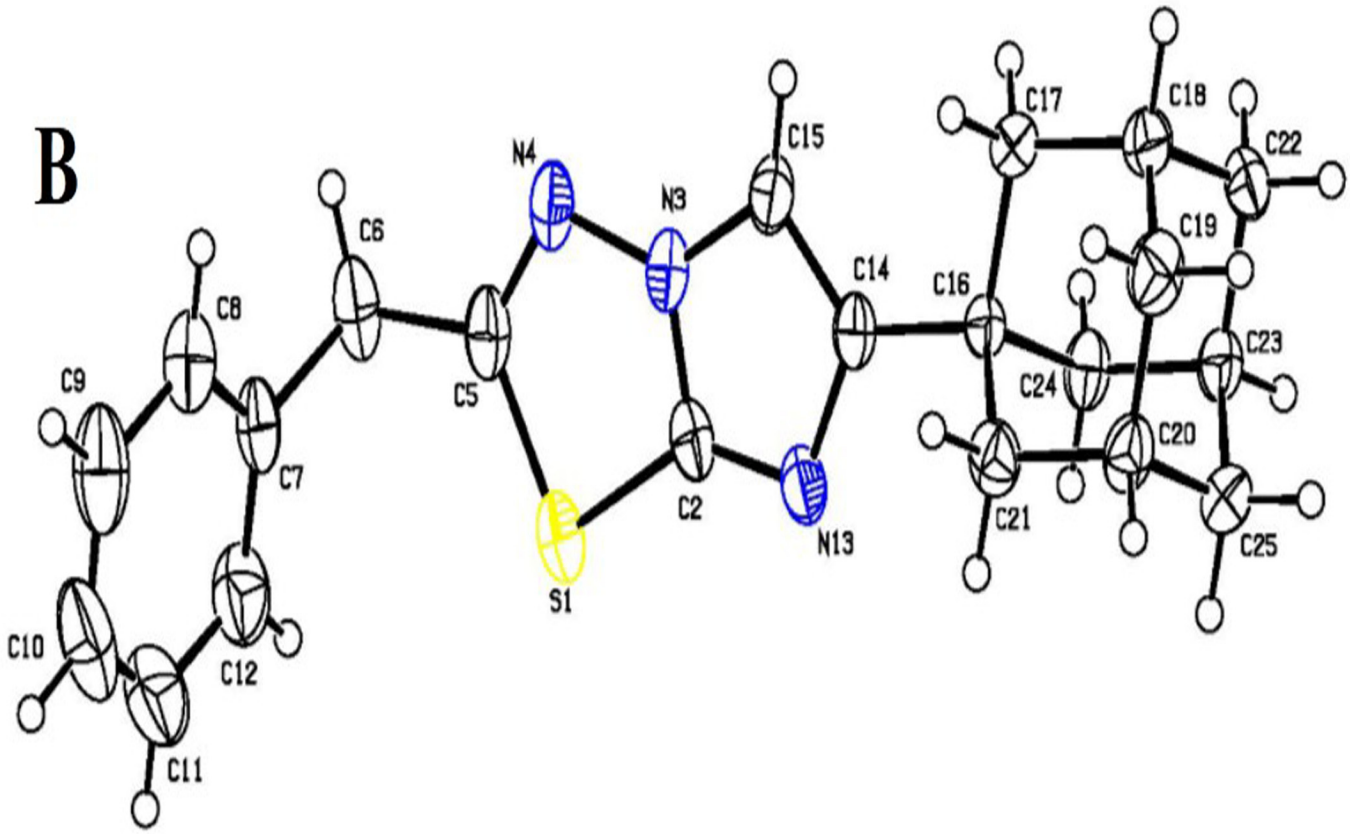

Fig 1. A) Schematic representation of the preparation of AITs. B) ORTEP diagram of 3b. The compound crystallizes in a triclinic system under the space group P-1, and the benzyl imidazothiadiazole moiety adopts a chair conformation with the benzyl imidazothiadiazole moiety and the phenyl ring being bridged by the carbon atom (C6) with a dihedral angle of 69.73 degrees.

doi:10.1371/journal.pone.0139798.g001

Anti-TB activity of novel AITs

The *in vitro* Alamar Blue assay was employed to determine the Anti-TB activity of AITs against the *M*. *tuberculosis* H_{37}Rv strain as described earlier [29]. Various concentrations of AITs were added to the culture of *M*. *tuberculosis* and minimum inhibitory concentrations (MIC) of AITs were measured and the results are tabulated in Table 2. Most AITs showed inhibitory activity towards the *M*. *tuberculosis* H_{37}Rv strain, suggesting that AITs possess significant anti-TB activity. Notably, Compound **3a, 3f,** and **3i** dispalyed relatively low MIC values of 10.5, 8.5 and 12.5 μM respectively when compared to the other structurally related compounds. Compounds with electron-donating phenyl, 4-methoxy phenyl, and methyl substituents attached to the imidazo-thiadiazole scaffold were favorable for activity against *M*. *tuberculosis*.

In silico molecular interactions of AITs towards sterol 14α-demethylase

As sterol 14α-demethylase (CYP51) is known to process a variety of sterols and as a drug target in *M*. *tubercolosis* [30, 31], we attempted to rationalize the anti-TB activity of the AITs synthesized in this work on a structural basis. Therefore, we docked all AITs to the X-ray structure of *M*. *tubercolosis* CYP51 in complex with a small molecule inhibitor (PDB: 2CIB) [32] using MOE default settings (Fig 2A) [33] and visualized predicted protein-ligand interactions with Pymol [34]. It was found that the imidazo-thiadiazole scaffold of **3f** likely interacts with the heme co-factor of CYP51 (see Fig 2B). Furthermore, the hydrophobic moieties are positioned in similar positions to the ring centers found in the co-crystallized ligand. Based on this analysis, CYP51 appeared to be a plausible target for AITs on a structure-based level. Further, in order to analyze the similarities in binding mode between AITs, we superposed the ligand in the co-crystal used for docking with compound **3a** using MOE's flexible alignment module and default settings [33]. We found an almost perfect shape overlap of the lowest energy conformations of AITs with all hydrophobic centers coinciding with the co-cyrstallized ligand (see Fig 2C). Therefore, the AITs

Table 1. Cyclocondensation of 5-Phenyl-2-amino-1,3,4-thiadiazole (2) with 1-Adamantyl bromomethylketone (1) under various reaction conditions to form title compounds. It can be seen that using nano-MgO as a base and employing ionic liquids instead of traditional organic solvents considerably increase yields above 90%.

Entry	Reaction conditions	Reaction time (h)	Yield (%)
1	Ethanol[a] / Na_2CO_3	36	37
2	1-Butanol[b] / MgO	42	38
3	N,N-DMF[c] /Et_3N	30	30
4	1-Butyl-3-methyl imidazolium tetrafluoroborate[d]/ Na_2CO_3	25	68
5	1-Butyl-4-methyl pyridinium hexafluorophosphate[d]/ K_2CO_3	24	55
6	1-Butyl-3-methyl imidazolium tetrafluoroborate[d]/ Et_3N	24	58
7	1-Butyl-4-methyl pyridinium hexafluorophosphate[d]/ MgO	14	64
8	1-Butyl-3-methyl imidazolium tetrafluoroborate[d]/ MgO	11	71
9	1-Butyl-3-methyl imidazolium tetrafluoroborate[d]/Nano MgO	3	93
10	1-Butyl-4-methyl pyridinium hexafluorophosphate[d]/ Nano MgO	3	95

[a]Reaction temperature = 80°C

[b]Reaction temperature = 95°C

[c]Reaction temperature = 120°C

[d]Reaction temperature = 60°C.

doi:10.1371/journal.pone.0139798.t001

Table 2. Cyclocondensation of 5-alkyl/aryl-2-amino-1,3,4-thiadiazole (1a-j) with 1-adamantyl bromomethylketone to form (3a-j).

Entry	R	Product (3a-j)	Reaction time (h)	Yield (%)	Melting point (°C)	Alamar Blue Activity (μM)
3a	C_6H_5	6-(adamantan-1-yl)-2-phenylimidazo[2,1-b][1,3,4] thiadiazole	3	83	142	10.5
3b	$CH_2C_6H_5$	6-(adamantan-1-yl)-2-benzylimidazo[2,1-b][1,3,4] thiadiazole	2	79	112	30.7
3c	4-NO_2- C_6H_4	6-(adamantan-1-yl)-2-(4-nitrophenyl)imidazo[2,1-b] [1,3,4]thiadiazole	3	79	163	28.7
3d	4-OCH_3-$C_6H_4CH_2$	6-(adamantan-1-yl)-2-(4-methoxybenzyl)imidazo [2,1-b][1,3,4]thiadiazole	2	86	126	32.7
3e	C_4H_3O	6-(adamantan-1-yl)-2-(furan-2-yl)imidazo[2,1-b] [1,3,4]thiadiazole	2	77	131	38.2
3f	4-OCH_3-C_6H_4	6-(adamantan-1-yl)-2-(4-methoxyphenyl)imidazo [2,1-b][1,3,4]thiadiazole	2	84	157	8.5
3g	4-Br-C_6H_4	6-(adamantan-1-yl)-2-(4-bromophenyl)imidazo [2,1-b][1,3,4]thiadiazole	3	81	161	20.0
3h	C_6H_{11}	6-(adamantan-1-yl)-2-cyclohexylimidazo[2,1-b] [1,3,4]thiadiazole	2	74	198	36.5
3i	CF_3	6-(adamantan-1-yl)-2-(trifluoromethyl)imidazo [2,1-b][1,3,4]thiadiazole	2	63	>300	12.0
3j	CH_3	6-(adamantan-1-yl)-2-methylimidazo[2,1-b][1,3,4] thiadiazole	2	67	203	22.7
Pyrazinamide						12.5
Streptomycin						5.3
Ciprofloxacin						4.5

Equimolar mixture of **1a-j**, and **2** was dissolved in 2 ml of $[BMIM]^+[BF_4]^-$ and the reaction was carried out in the presence of 0.1 equivalent of **Nano** MgO at 60 ^{0}C.

doi:10.1371/journal.pone.0139798.t002

presented in this work could be considered a continuation of the 1,3,4-thiadizole series presented earlier by Oruc et al. [16] including an isosteric replacement of the core ring fragment.

In vitro anti-microbial activity of AITs against fungal strains that express 14α-demethylase (CYP51)

Our *in vitro* and *in silico* studies revealed that AITs showed good anti-TB activity at the low micro molar concentrations, and by plausibly targeting sterol 14α-demethylase (CYP51). In order to find further experimental support for the mode-of-action analysis of the AITs presented here, the CM237 and akuB strains *of A. fumigatus* that express CYP51 were selected for the next step. We further investigated the effect of AITs at various concentrations against both the fungal strains by broth microdilution method as reported previously [35]. MICs were determined visually in duplicate and recorded after 48 h. Results are summarized in Table 3. Interestingly, the most active compounds against *M. tuberculosis*, namely **3a, 3f,** and **3i** also exhibited significant inhibitory effect against the tested *A. fumigates* strains. These results lend further support–though not definite proof to their plausible mode-of-action by targeting sterol 14α-demethylase (CYP51).

Materials and Methods

All solvents used were of analytical grade and reagents used were purchased from Sigma-Aldrich chemicals. All IR spectra were obtained in a KBr disc on a Shimadzu FT-IR 157 Spectrometer. ^{1}H and ^{13}C NMR spectra were recorded on a Bruker WH-200 (400 MHz) in $CDCl_3$

Figure 2

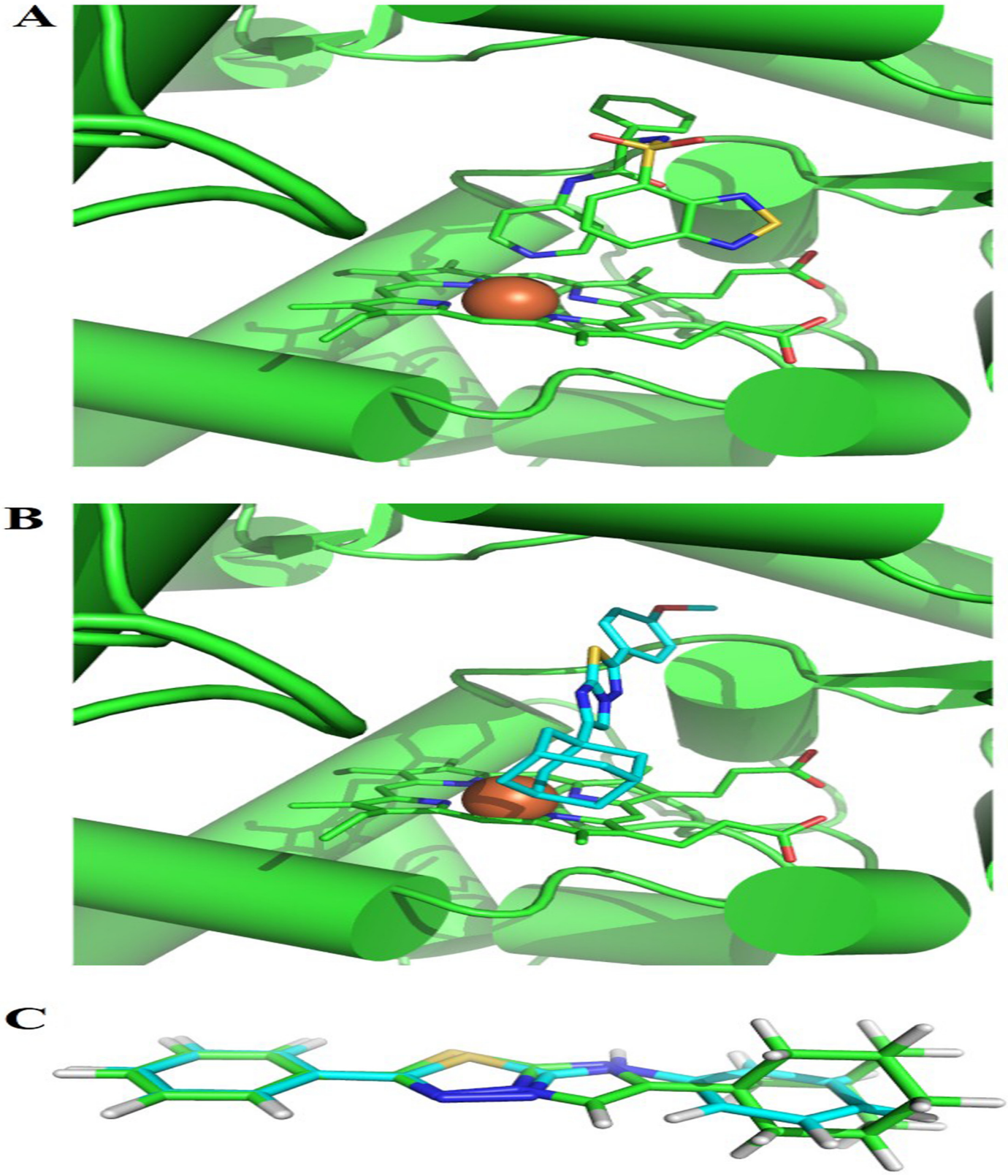

Fig 2. Computational binding mode analysis of AITs and *M. tubercolosis* CYP51. A) X-ray structure of CYP51 (green cartoon representation with heme cofactor as sticks with bound iron as brown sphere) in complex with a small molecule inhibitor (PDB: 2CIB). B) Similar interactions and an analogous three-dimensional arrangement are shown for compound **3f** of the AITs (cyan sticks). C) Overlay of the parent 1,3,4-thiadiazole of Oruc et al [Oruc04] with compound **3a** of the AITs. Positioning of ring centers, exit vectors, and overall shape are very similar, thereby plausibly explaining a similar bioactivity profile.

doi:10.1371/journal.pone.0139798.g002

or DMSO-d_6 as solvent, using tetramethylsilane (TMS) as an internal standard and chemical shifts are expressed as ppm. Mass spectra were determined on a Shimanzu LC-MS. The elemental analyses were carried out using an Elemental Vario Cube CHNS rapid Analyzer. The progress of the reaction was monitored by TLC pre-coated silica gel G plates.

Typical procedure for the synthesis of AITs

A mixture of 5-alkyl/aryl-2-amino1,3,4-thiadiazole (0.01 mol), 1-adamantyl bromomethylketone (0.01 mol) and nano magnesium oxide (0.001 mol) in 2 ml of 1-Butyl-3-methylimidazolium tetrafluoroborate $[BMIM]^+[BF_4]^-$ was stirred at 60°C for the appropriate time (Table 2). After completion of the reaction, as determined by TLC, the reaction mixture was cooled down and then quenched into ice water. The product was extracted from the water layer by 3×5 mL diethyl ether, dried with magnesium sulfate, filtered, and concentrated *in vacuo*. The crude product was purified by chromatography employing a column of 30 mm diameter using 60–120 silica gel and hexane/ethyl acetate (80:20) as mobile phase. All new compounds exhibited spectral properties consistent with the assigned structures (S2 Data).

***6-(Adamantan-1-yl)-2-phenylimidazo[2,1-b][1,3,4]thiadiazole (3a)*:** ^{1}H NMR (400 MHz, $CDCl_3$) δ: 8.0 (s, 1H), 7.8 (m, 2H), 7.6 (m, 2H), 7.4 (m, 1H), 2.1 (m, 6H), 1.9 (m, 3H), 1.7 (m,6H); ^{13}C NMR ($CDCl_3$): 175.73, 134.92, 133.26, 132.17,129.39, 128.09, 127.56, 123.43, 45.59, 42.75, 38.19, 28.48; LCMS (MM:ES+APCI) 336.3 $(M+H)^+$; Anal.Calcd for $C_{20}H_{21}N_3S$: C 71.61; H 6.31; N 12.53. Found: C, 71.43; H, 6.47; N, 12.66.

***6-(Adamantan-1-yl)-2-benzylimidazo[2,1-b][1,3,4]thiadiazole (3b)*:** ^{1}H NMR (400 MHz, $CDCl_3$) δ: 8.0 (s, 1H), 7.4 (m, 2H), 7.3 (m, 3H), 4.4 (s, 2H), 1.7–2.2 (m,15H); ^{13}C NMR ($CDCl_3$); 161.09, 135.82, 134.73, 129.04, 128.23, 125.56, 123.65, 45.56, 42.78, 38.65, 38.32, 28.66; LCMS (MM:ES+APCI) 350.3$(M+H)^+$; Anal. Calcd for $C_{21}H_{23}N_3$: C, 72.17; H, 6.63; N, 12.02. Found: C, 71.98; H, 6.78; N 12.24.

***6-(Adamantan-1-yl)-2-(4-nitrophenyl)imidazo[2,1-b][1,3,4]thiadiazole (3c)*:** ^{1}H NMR (400 MHz, $CDCl_3$) δ: 8.1 (d, 2H), 8.0 (s, 1H), 7.9 (d, 2H), 2.1(m,6H),1.9(m, 3H), 1.7(m,6H); ^{13}C NMR ($CDCl_3$); 175.64, 148.97, 139.92, 135.33, 134.83, 128.65, 123.34, 121.78, 45.56, 42.78, 38.12, 28.55; LCMS (MM:ES+APCI) 381.2 $(M+H)^+$; Anal. Calcd for $C_{20}H_{20}N_4O_2S$: C, 63.14; H, 5.30; N, 14.73. Found: C, 63.18; H, 5.88; N, 13.89.

***6-(Adamantan-1-yl)-2-(4-methoxybenzyl)imidazo[2,1-b][1,3,4]thiadiazole (3d)*:** ^{1}H NMR (400 MHz, $CDCl_3$) δ: 8.0 (s, 1H), 7.9 (d, 2H), 7.6 (d, 2H), 4.3 (s, 3H), 4.0 (s, 2H), 2.1 (m, 6H),1.9(m, 3H), 1.7(m, 6H); ^{13}C NMR ($CDCl_3$); 161.06, 159.43, 135.92, 134.83, 130.33, 128.23, 123.45, 114.45, 55.89, 45.56, 42.78, 38.22, 28.51; LCMS (MM:ES+APCI) 380.2 $(M+H)^+$; Anal. Calcd for $C_{22}H_{25}N_3OS$: C, 69.62; H, 6.64; N, 11.07. Found: C, 69.48; H, 7.03; N, 11.86.

***6-(Adamantan-1-yl)-2-(furan-2-yl)imidazo[2,1-b][1,3,4]thiadiazole (3e)*:** ^{1}H NMR (400 MHz, $CDCl_3$) δ: 8.1 (d, 1H), 8.00 (s, 1H), 7.4 (d, 2H), 6.8 (t, 1H), 2.1 (m, 6H), 1.9 (m, 3H),

Table 3. MIC values obtained from the lead AIT compounds against *A. fumigates*, which expresses CYP51. Given the activity of compounds in this system this finding corroborates CYP51 as a plausible target of the AIT series.

Aspergillus fumigatus strain	Compound 3a MIC (μg/ml)	Compound 3f MIC (μg/ml)	Compound 3i MIC (μg/ml)
WT 237	16	16	16
WT akuB	8	8	8

doi:10.1371/journal.pone.0139798.t003

1.7 (m, 6H); ^{13}C NMR ($CDCl_3$); 146.29, 142.97, 135.92, 134.83, 123.65, 107.45, 105.66, 45.56, 42.78, 38.22, 28.51; LCMS (MM:ES+APCI) 326.3 $(M+H)^+$; Anal. Calcd for $C_{18}H_{19}N_3OS$: C, 66.43; H, 5.88; N, 12.91. Found: C, 65.83; H, 6.05; N, 13,44.

***6-(Adamantan-1-yl)-2-(4-methoxyphenyl)imidazo[2,1-b][1,3,4]thiadiazole (3f)*:** ^{1}H NMR (400 MHz, $CDCl_3$) δ: 8.2 (d, J = 8.4 Hz, 1H), 8.00 (s, 1H), 7.8 (d, 2H), 4.4 (s, 3H), 2.1 (m,6H), 1.9–1.7(m,9H); ^{13}C NMR ($CDCl_3$); 175.11, 160.63, 135.99, 134.83, 128.79, 125.32, 123.65, 114.45, 55.79, 45.56, 42.78, 38.22, 28.51; LCMS (MM:ES+APCI) 366.6 $(M+H)^+$; Anal. Calcd for $C_{21}H_{23}N_3OS$: C, 69.01; H, 6.34; N, 11.50. Found: C, 68.33; H, 5.89; N,11.10.

***6-(Adamantan-1-yl)-2-(4-bromophenyl)imidazo[2,1-b][1,3,4]thiadiazole (3g)*:** ^{1}H NMR (400 MHz, $CDCl_3$) δ: 8.3 (d, 2H), 8.1 (d, 2H), 8.0 (s, 1H), 2.0 (m, 6H),1.8 (m, 3H), 1.6 (m, 6H); ^{13}C NMR ($CDCl_3$); 175.14, 135.92, 134.87, 132.36, 129.56, 123.65, 45.57, 42.78, 38.29, 28.55; LCMS (MM:ES+APCI) 415.1 $(M+H)^+$; Anal. Calcd for $C_{20}H_{20}BrN_3S$: C, 57.97; H, 4.87; N, 10.14. Found: C, 57.01; H, 4,22; N, 9.56.

***6-(Adamantan-1-yl)-2-cyclohexylimidazo[2,1-b][1,3,4]thiadiazole (3h)*:** ^{1}H NMR (400 MHz, $CDCl_3$) δ: 8.0 (s, 1H), 2.7 (m, 2H), 2.1–1.8 (m, 15H), 1.7 (m, 6H), 1.5–1.4 (m, 3H); ^{13}C NMR ($CDCl_3$); 135.89, 134.88, 123.67, 45.61, 42.83, 38.29, 33.27, 28.58, 27.95, 25.46; LCMS (MM:ES+APCI) 342.3 $(M+H)^+$; Anal. Calcd for $C_{20}H_{27}N_3S$: C, 70.34; H, 7.97; N, 12.30. Found: C, 70.87; H, 8.54; N, 11.67.

***6-(Adamantan-1-yl)-2-(trifluoromethyl)imidazo[2,1-b][1,3,4]thiadiazole (3i)*:** ^{1}H NMR (400 MHz, $CDCl_3$) δ: 8.0 (s, 1H), 2.1 (m,6H),1.9 (m, 3H), 1.7 (m,6H); ^{13}C NMR ($CDCl_3$); 135.92, 134.88, 123.55, 45.54, 42.72, 38.21, 28.54, 17.34; LCMS (MM:ES+APCI) 328.4$(M+H)^+$; Anal. Calcd for $C_{15}H_{16}F_3N_3S$: C, 55.03; H, 4.93; N, 12.84. Found: C, 55.37; H, 4.44; N, 12.13.

***6-(Adamantan-1-yl)-2-methylimidazo[2,1-b][1,3,4]thiadiazole (3j)*:** ^{1}H NMR (400 MHz, $CDCl_3$) δ: 8.0 (s, 1H), 2.8 (s, 3H), 2.1 (m,6H), 1.9 (m, 3H), 1.7 (m,6H); ^{13}C NMR ($CDCl_3$); 157.89, 135.92, 134.83, 123.65, 118.45, 45.56, 42.78, 38.22, 28.51; LCMS (MM:ES+APCI) 274.4 $(M+H)^+$; Anal. Calcd for $C_{18}H_{14}FNO$: C, 65.90; H, 7.00; N, 15.37. Found: C, 66.09; H, 7.65; N, 15.89.

X-ray crystal structure determination of (3b)

A single crystal of compound **3b** with dimensions of 0.30 × 0.25 × 0.20 mm was chosen for X-ray diffraction studies. The data were collected on a Bruker SMART APEX II X-ray diffractometer with Cu Kα radiation. Raw data was processed and reduced by using APEX2 and SAINT [36, 37]. The crystal structure was solved by direct methods using SHELXS-97 [38]. All non-hydrogen atoms were revealed in the first Fourier map itself. Anisotropic refinement of non-hydrogen atoms was started at this stage. Subsequent refinements were carried out with anisotropic thermal parameters for non-hydrogen atoms and isotropic temperature factors for the hydrogen atoms which were placed at chemically acceptable positions. Full-matrix least squares refinement was carried out using SHELXL-97 [39] with a final residual value of R1 = 0.079. The thermal ellipsoid plot [40] of the molecule at 50% probability is represented in Fig 1B. The details of crystallographic information have been deposited at the CCDC with number 1056579.

The crystal structure analysis showed that the compound **3b** crystallizes in a triclinic system under the space group *P-1*, with cell parameters a = 6.3060(5) Å, *b* = 10.4279(7) Å, *c* = 14.1099 (10) Å, α = 81.101(2)°, β = 79.845(2)°, γ = 82.918(2)° and *Z* = 2. The benzyl imidazothiadiazole moiety adopts a chair conformation with puckering parameters Q = 0.622(4) Å and φ = 201(19)° [31] and the maximum deviation found on the puckered atom at C14 is 0.255(3) Å. The benzyl imidazothiadiazole moiety and the phenyl ring are bridged by the carbon atom (C6) with a dihedral angle of 69.73(5)°. The structure does not contain any classical hydrogen bonds.

Anti-tubercular activity assay

All the novel AITs were screened for anti-tubercular activity against *M*. *tuberculosis* $H_{37}Rv$ strain (ATCC 27294) using a microplate Alamar Blue assay (MABA) as described previously [29, 31]. Briefly, 200 μl of sterile deionized water was added to all outer-perimeter wells of sterile 96-well plates to minimize evaporation of the medium in the test wells during incubation. The wells in rows B to G in columns 3 to 11 received 100 μl of Middlebrook 7H9 broth. 100 μl of 2X drug solutions were added to the wells in rows B to G in columns 2. 100 μl was transferred from column 2 to column 3, and the contents of the wells were mixed well. Identical serial 1:2 dilutions were continued through column 10, and 100 μl of excess medium was discarded from the wells in column 10 in order to get the final concentration of 0.2 μg/ml. 100 μl of *M*. *tuberculosis* inoculum was added to the wells in rows B to G in columns 2 to 11 (yielding a final volume of 200 μl per well). Thus, the wells in column 11 served as drug-free control. The plate was sealed with parafilm and incubated at 37°C for 5 days. Thereafter, 50 μl of freshly prepared 1:1 mixture of Alamar Blue reagent and 10% tween-80 was added to each well and incubated for 24 h. Appearance of blue color was interpreted as no bacterial growth, and pink color was used as indicator of bacterial growth. The inhibitory activity of AITs against *M*. *tuberculosis* was expressed as the minimum inhibitory concentration (MIC) in μM. MIC was defined as lowest drug concentration which prevented the color change from blue to pink. Pyrazinamide, streptomycin, and ciprofloxacin were used as a positive controls.

Molecular docking analysis

In silico molecular docking was performed based on the X-ray structure of *M*. *tubercolosis* CYP51 in complex with a small molecule inhibitor (PDB: 2CIB) [32]. The ligand structures were energy-minimized and protonated using the MOE platform [33]. The protein was prepared for docking using protonate3D [41]. Afterwards, we docked all AITs to the X-ray structure of using MOE's default settings for flexible docking. This includes an initial placement using Triangle Matcher, primary scoring via London dG and a forcefield refinement of 30 poses followed by a re-scoring step using GBVI/WSA dG. We visualized predicted protein-ligand interactions with pymol [34].

Anti-microbial activity

The CM237 and akuB strains *of Aspergillus fumigatus*, that expresses CYP51, were used in this work. Fungal strains were grown in Potato Dextrose Agar (PDA, Becton Dickinson, Madrid, Spain) at 37°C. After three days of growth a suspension of spores was prepared by harvesting the surface of the culture with phosphate buffered saline (PBS) plus 0.01% Tween 20. Inoculum size was then adjusted using a hemocytometer chamber according to needs. Stock solutions of each compound were first dissolved in chloroform and subjected to serial dilution to obtain the concentrations of 64, 32, 16, 8, 4, 2, 1, 0.5, 0.25 and 0.125 μg/ml. Each compound was tested between 64 μg/ml and 0.125 μg/ml. Compounds susceptibility was determined by broth microdilution (BMD) using RPMI 2% glucose. MICs were determined visually and recorded after 48 h. Amphotericin B and chloroform were used as controls of the study.

Conclusion

In this work, we synthesized novel AITs using 1-adamantyl bromomethylketone and 5-alkyl/aryl-2-amino1,3,4-thiadiazoles employing nano-MgO in ionic liquid media. We experimentally confirmed the anti-TB activity of all AITs against *M*. *tuberculosis* $H_{37}Rv$ strain with MICs in the low micromolar range. Subsequent docking studies revealed sterol 14α-demethylase

(CYP51) as a plausible target, and subsequent activity determination against fungal strains that express sterol 14α-demethylase (CYP51) corroborated this hypothesis. In summary, we herein report the synthesis and anti-TB activity of novel AITs that likely target sterol 14α-demethylase (CYP51) to induce their antimycobacterial activity.

Supporting Information

S1 Data. Graphical abstract which provides the overview of the present work.
(DOCX)

S2 Data. Scanned spectral images and structural analysis of novel adamantyl-imidazolo-thiadiazole derivatives.
(DOCX)

Acknowledgments

This research was supported by University Grants Commission (41-257-2012-SR), Vision Group Science and Technology, Department of Science and Technology (NO. SR/FT/LS-142/2012). KSR thanks Institution of Excellence, University of Mysore for funding. AB thanks Unilever and the European Research Commission (ERC Starting Grant 2013) for funding. SP thanks the Netherlands Organization for Scientific Research (NWO, grant number NWO-017.009–065) and the Prins Bernhard Cultuurfonds for funding. CDM thanks University of Mysore for Department of Science and Technology-Promotion of University Research and Scientific Excellence (DST-PURSE) Research Associate fellowship. We thank Emilia Mellado for providing the experimental data that related to antifungal studies.

Author Contributions

Conceived and designed the experiments: B KSR AB. Performed the experiments: SA BRCP SR SM C SP LM JEF B CDM. Analyzed the data: MM CDM JM AB B KSR. Contributed reagents/materials/analysis tools: AB B KSR MM. Wrote the paper: B AB KSR.

References

1. Du Toit LC, Pillay V, Danckwerts MP. Tuberculosis chemotherapy: current drug delivery approaches. Respir Res. 2006; 7(1):118.
2. Addla D, Jallapally A, Gurram D, Yogeeswari P, Sriram D, Kantevari S. Design, synthesis and evaluation of 1,2,3-triazole-adamantylacetamide hybrids as potent inhibitors of Mycobacterium tuberculosis. Bioorganic & medicinal chemistry letters. 2014; 24(8):1974–9. Epub 2014/04/01. doi: 10.1016/j.bmcl.2014.02.061 PMID: 24679703.
3. Berg J, Blumberg EJ, Sipan CL, Friedman LS, Kelley NJ, Vera AY, et al. Somatic complaints and isoniazid (INH) side effects in Latino adolescents with latent tuberculosis infection (LTBI). Patient education and counseling. 2004; 52(1):31–9. Epub 2004/01/20. PMID: 14729288.
4. Xia YY, Hu DY, Liu FY, Wang XM, Yuan YL, Tu de H, et al. Design of the anti-tuberculosis drugs induced adverse reactions in China National Tuberculosis Prevention and Control Scheme Study (ADACS). BMC public health. 2010; 10:267. Epub 2010/05/25. doi: 10.1186/1471-2458-10-267 PMID: 20492672; PubMed Central PMCID: PMCPmc2893093.
5. Bocanegra-García V, García A, Rivera G, Palos I, Palma-Nicolás JP. Antitubercular drugs development: recent advances in selected therapeutic targets and rational drug design: INTECH Open Access Publisher; 2011.
6. Balderas-Renteria I, Gonzalez-Barranco P, Garcia A, Banik BK, Rivera G. Anticancer drug design using scaffolds of beta-lactams, sulfonamides, quinoline, quinoxaline and natural products. Drugs advances in clinical trials. Current medicinal chemistry. 2012; 19(26):4377–98. Epub 2012/06/20. PMID: 22709002.
7. Menezes CM, Rivera G, Alves MA, do Amaral DN, Thibaut JP, Noel F, et al. Synthesis, biological evaluation, and structure-activity relationship of clonazepam, meclonazepam, and 1,4-benzodiazepine

compounds with schistosomicidal activity. Chemical biology & drug design. 2012; 79(6):943–9. Epub 2012/02/11. doi: 10.1111/j.1747-0285.2012.01354.x PMID: 22321778.

8. Wanka L, Iqbal K, Schreiner PR. The lipophilic bullet hits the targets: medicinal chemistry of adamantane derivatives. Chemical reviews. 2013; 113(5):3516–604. Epub 2013/02/26. doi: 10.1021/cr100264t PMID: 23432396; PubMed Central PMCID: PMCPmc3650105.
9. Scherman MS, North EJ, Jones V, Hess TN, Grzegorzewicz AE, Kasagami T, et al. Screening a library of 1600 adamantyl ureas for anti-Mycobacterium tuberculosis activity in vitro and for better physical chemical properties for bioavailability. Bioorganic & medicinal chemistry. 2012; 20(10):3255–62. Epub 2012/04/24. doi: 10.1016/j.bmc.2012.03.058 PMID: 22522007; PubMed Central PMCID: PMCPmc3345085.
10. Sacksteder KA, Protopopova M, Barry CE 3rd, Andries K, Nacy CA. Discovery and development of SQ109: a new antitubercular drug with a novel mechanism of action. Future microbiology. 2012; 7 (7):823–37. Epub 2012/07/26. doi: 10.2217/fmb.12.56 PMID: 22827305; PubMed Central PMCID: PMCPmc3480206.
11. Makobongo MO, Einck L, Peek RM Jr., Merrell DS. In vitro characterization of the anti-bacterial activity of SQ109 against Helicobacter pylori. PloS one. 2013; 8(7):e68917. Epub 2013/08/13. doi: 10.1371/journal.pone.0068917 PMID: 23935905; PubMed Central PMCID: PMCPmc3723868.
12. Jia L, Tomaszewski JE, Hanrahan C, Coward L, Noker P, Gorman G, et al. Pharmacodynamics and pharmacokinetics of SQ109, a new diamine-based antitubercular drug. British journal of pharmacology. 2005; 144(1):80–7. Epub 2005/01/13. doi: 10.1038/sj.bjp.0705984 PMID: 15644871; PubMed Central PMCID: PMCPmc1575972.
13. Koser CU, Javid B, Liddell K, Ellington MJ, Feuerriegel S, Niemann S, et al. Drug-resistance mechanisms and tuberculosis drugs. Lancet (London, England). 2015; 385(9965):305–7. Epub 2015/02/24. doi: 10.1016/s0140-6736(14)62450-8 PMID: 25706840; PubMed Central PMCID: PMCPmc4374148.
14. Kolavi G, Hegde V, Khazi I, Gadad P. Synthesis and evaluation of antitubercular activity of imidazo[2,1-b][1,3,4]thiadiazole derivatives. Bioorganic & medicinal chemistry. 2006; 14(9):3069–80. Epub 2006/01/13. doi: 10.1016/j.bmc.2005.12.020 PMID: 16406644.
15. Sink R, Sosic I, Zivec M, Fernandez-Menendez R, Turk S, Pajk S, et al. Design, synthesis, and evaluation of new thiadiazole-based direct inhibitors of enoyl acyl carrier protein reductase (InhA) for the treatment of tuberculosis. Journal of medicinal chemistry. 2015; 58(2):613–24. Epub 2014/12/18. doi: 10.1021/jm501029r PMID: 25517015.
16. Oruc EE, Rollas S, Kandemirli F, Shvets N, Dimoglo AS. 1,3,4-thiadiazole derivatives. Synthesis, structure elucidation, and structure-antituberculosis activity relationship investigation. Journal of medicinal chemistry. 2004; 47(27):6760–7. Epub 2004/12/24. doi: 10.1021/jm0495632 PMID: 15615525.
17. Basappa, Sadashiva MP, Mantelingu K, Swamy SN, Rangappa KS. Solution-phase synthesis of novel delta2-isoxazoline libraries via 1,3-dipolar cycloaddition and their antifungal properties. Bioorganic & medicinal chemistry. 2003; 11(21):4539–44. Epub 2003/10/07. PMID: 14527549.
18. Kavitha CV, Basappa, Swamy SN, Mantelingu K, Doreswamy S, Sridhar MA, et al. Synthesis of new bioactive venlafaxine analogs: novel thiazolidin-4-ones as antimicrobials. Bioorganic & medicinal chemistry. 2006; 14(7):2290–9. Epub 2005/12/13. doi: 10.1016/j.bmc.2005.11.017 PMID: 16338140.
19. Priya BS, Basappa, Swamy SN, Rangappa KS. Synthesis and characterization of novel 6-fluoro-4-piperidinyl-1,2-benzisoxazole amides and 6-fluoro-chroman-2-carboxamides: antimicrobial studies. Bioorganic & medicinal chemistry. 2005; 13(7):2623–8. Epub 2005/04/26. PMID: 15846867.
20. Keerthy HK, Garg M, Mohan CD, Madan V, Kanojia D, Shobith R, et al. Synthesis and characterization of novel 2-amino-chromene-nitriles that target Bcl-2 in acute myeloid leukemia cell lines. PloS one. 2014; 9(9):e107118. Epub 2014/10/01. doi: 10.1371/journal.pone.0107118 PMID: 25268519; PubMed Central PMCID: PMCPmc4182326.
21. Anusha S, Anandakumar B, Mohan CD, Nagabhushana G, Priya B, Rangappa KS. Preparation and use of combustion-derived Bi 2 O 3 for the synthesis of heterocycles with anti-cancer properties by Suzuki-coupling reactions. RSC Advances. 2014; 4(94):52181–8.
22. Neelgundmath M, Dinesh KR, Mohan CD, Li F, Dai X, Siveen KS, et al. Novel synthetic coumarins that targets NF-kappaB in Hepatocellular carcinoma. Bioorganic & medicinal chemistry letters. 2015; 25 (4):893–7. Epub 2015/01/17. doi: 10.1016/j.bmcl.2014.12.065 PMID: 25592709.
23. Rakesh KS, Jagadish S, Vinayaka AC, Hemshekhar M, Paul M, Thushara RM, et al. A new ibuprofen derivative inhibits platelet aggregation and ROS mediated platelet apoptosis. PloS one. 2014; 9(9): e107182. Epub 2014/09/23. doi: 10.1371/journal.pone.0107182 PMID: 25238069; PubMed Central PMCID: PMCPmc4169656.
24. Bharathkumar H, Mohan CD, Ananda H, Fuchs JE, Li F, Rangappa S, et al. Microwave-assisted synthesis, characterization and cytotoxic studies of novel estrogen receptor alpha ligands towards human

breast cancer cells. Bioorganic & medicinal chemistry letters. 2015; 25(8):1804–7. Epub 2015/03/24. doi: 10.1016/j.bmcl.2015.01.030 PMID: 25797502.

25. Bharathkumar H, Paricharak S, Dinesh KR, Siveen KS, Fuchs JE, Rangappa S, et al. Synthesis, biological evaluation and in silico and in vitro mode-of-action analysis of novel dihydropyrimidones targeting PPAR-[gamma]. RSC Advances. 2014; 4(85):45143–6. doi: 10.1039/C4RA08713E

26. Tang Z-X, Lv B-F. MgO nanoparticles as antibacterial agent: preparation and activity. Brazilian Journal of Chemical Engineering. 2014; 31(3):591–601.

27. Reddy MM, Ashoka S, Chandrappa G, Pasha M. Nano-MgO: an efficient catalyst for the synthesis of formamides from amines and formic acid under MWI. Catalysis letters. 2010; 138(1–2):82–7.

28. Welton T. Room-temperature ionic liquids. Solvents for synthesis and catalysis. Chemical reviews. 1999; 99(8):2071–84. PMID: 11849019

29. Reis RS, Neves I Jr., Lourenco SL, Fonseca LS, Lourenco MC. Comparison of flow cytometric and Alamar Blue tests with the proportional method for testing susceptibility of Mycobacterium tuberculosis to rifampin and isoniazid. Journal of clinical microbiology. 2004; 42(5):2247–8. Epub 2004/05/08. PMID: 15131202; PubMed Central PMCID: PMCPmc404654.

30. Chen CK, Doyle PS, Yermalitskaya LV, Mackey ZB, Ang KK, McKerrow JH, et al. Trypanosoma cruzi CYP51 inhibitor derived from a Mycobacterium tuberculosis screen hit. PLoS neglected tropical diseases. 2009; 3(2):e372. Epub 2009/02/05. doi: 10.1371/journal.pntd.0000372 PMID: 19190730; PubMed Central PMCID: PMCPmc2629123.

31. Franzblau SG, Witzig RS, McLaughlin JC, Torres P, Madico G, Hernandez A, et al. Rapid, low-technology MIC determination with clinical Mycobacterium tuberculosis isolates by using the microplate Alamar Blue assay. Journal of clinical microbiology. 1998; 36(2):362–6. Epub 1998/02/18. PMID: 9466742; PubMed Central PMCID: PMCPmc104543.

32. Podust LM, von Kries JP, Eddine AN, Kim Y, Yermalitskaya LV, Kuehne R, et al. Small-molecule scaffolds for CYP51 inhibitors identified by high-throughput screening and defined by X-ray crystallography. Antimicrobial agents and chemotherapy. 2007; 51(11):3915–23. Epub 2007/09/12. doi: 10.1128/aac.00311-07 PMID: 17846131; PubMed Central PMCID: PMCPmc2151439.

33. Molecular Operating Environment (MOE) CCGI, Montreal Q, Canada, 2013.

34. De Lano W: The Pymol Molecular Graphics System v, De Lano Scientific, San Carlos, CA.

35. Arendrup MC, Cuenca-Estrella M, Lass-Florl C, Hope WW. EUCAST technical note on Aspergillus and amphotericin B, itraconazole, and posaconazole. Clinical microbiology and infection: the official publication of the European Society of Clinical Microbiology and Infectious Diseases. 2012; 18(7):E248–50. Epub 2012/05/01. doi: 10.1111/j.1469-0691.2012.03890.x PMID: 22540149.

36. Bruker APEX2 and SAINT Bruker AXS Inc. Madison W, USA 2009.

37. Bruker AaSBAI, Madison, Wisconsin, USA 2009.

38. Hubschle CB, Sheldrick GM, Dittrich B. ShelXle: a Qt graphical user interface for SHELXL. Journal of applied crystallography. 2011; 44(Pt 6):1281–4. Epub 2012/04/06. doi: 10.1107/s0021889811043202 PMID: 22477785; PubMed Central PMCID: PMCPmc3246833.

39. Spek AL. Structure validation in chemical crystallography. Acta Crystallographica Section D: Biological Crystallography. 2009; 65(2):148–55.

40. Cremer Dt, Pople J. General definition of ring puckering coordinates. Journal of the American Chemical Society. 1975; 97(6):1354–8.

41. Labute P. Protonate3D: assignment of ionization states and hydrogen coordinates to macromolecular structures. Proteins. 2009; 75(1):187–205. Epub 2008/09/25. doi: 10.1002/prot.22234 PMID: 18814299; PubMed Central PMCID: PMCPmc3056144.